A Study of the Effect of Cross-Sectional Shape on the Sorting Flow Field of a Spiral Concentrator

Huizhong Liu[1,2,*], Ao Huang[1]

[1]School of Mechanical and Electrical Engineering, Jiangxi University of Science and Technology, Ganzhou, 341000, China
[2]Jiangxi Province Engineering Research Center for Mechanical and Electrical of Mining and Metallurgy, Ganzhou ,341000, China

*huizhong6@163.com; 1084804453@qq.com

Abstract. Spiral concentrator is a kind of fluid-film gravity concentrator, and the flow pattern of the slurry film in the spiral chute is closely related to the geometry of the spiral chute, especially the cross-sectional shape. In order to explore the influence of the cross-section shape of the spiral concentrator on the sorting flow pattern, this paper utilizes the CFD technology to construct three kinds of flow film with the cross-section shapes of "ellipse", "cubic parabola" and "composite curve", which are the same as that of the spiral concentrator. This paper uses CFD technology to construct three kinds of CFD models of "ellipse", "cubic parabola" and "composite curve", and with the help of the constructed model, the sorting flow state of the three kinds of cross-section shapes of spiral concentrator was analyzed and studied comparatively. The results show that the thickness and Reynolds number of the flow film at the inner edge of the spiral chute with elliptical cross-section are larger, which is more suitable for the loose and stratified sorting of coarse-grained minerals. The spiral chute with composite curve cross-section has a larger laminar flow area and a wider secondary circulation area, which is conducive to the sorting and recovery of fine-grained minerals.

Keywords: spiral concentrator; composite curvilinear cross section; CFD simulation; flow field characterization;

1 Introduction

As a kind of gravity concentrator, spiral concentrator is widely used in industrial production due to its advantages of low energy consumption, no pollution, high sorting efficiency and wide sorting range [1,2]. The sorting behavior of the spiral concentrator is directly related to the flow pattern of the slurry in the spiral chute, and the geometric structure parameters such as the cross-sectional shape of the spiral chute are closely related to the slurry flow pattern. Spiral concentrator was first invented by Humphrey in the United States, using elliptical cross-section curve [3]. But practice has proved that the elliptical cross-section spiral concentrator can not be adapted to the beneficia-

W. He et al. (eds.), *Proceedings of the 2024 10th International Conference on Advances in Energy Resources and Environment Engineering (ICAESEE 2024)*, Atlantis Highlights in Engineering 36,
https://doi.org/10.2991/978-94-6463-708-3_48

tion of fine-grained minerals in China [4].In 1974, the team of Fan Xiangbo developed the LL1200 spiral concentrator with the shape of the cross-section as a cubic paraboloid for the gravity beneficiation of fine-grained hematite in China, and achieved satisfactory sorting results, and then gained a large number of popularization in the industry. In order to distinguish from the elliptical cross-section shape of the spiral concentrator, our country called spiral chute. 1989 North Mining Institute of Li Kaigong team developed a "ellipse - straight line - parabolic" composite cross-section curve of the DL-2000 spiral concentrator, in the coarse particles of tin ore rougher to achieve good results. Studies have shown that the cross-section shape of the spiral chute is closely related to the distribution of the slurry in the radial direction of the spiral chute, the range and intensity of the secondary circulation, the flow velocity and other key flow characteristics, and will affect the sorting process of mineral particles accordingly. According to the existing application experience of our team, the elliptical spiral concentrator is generally suitable for the sorting of coarse-grained minerals, while the cubic parabolic shape is more suitable for the sorting of fine-grained minerals. Therefore, the study of the cross-section curve of the spiral concentrator is of great significance to improve the sorting performance of the spiral concentrator.

In recent years, the rapid development of computational fluid dynamics (CFD) technology has provided strong support for the qualitative and quantitative analysis of the flow field characteristics in spiral concentrators [5]. Zhu Hejun [6] utilized CFD technology to thoroughly study the relationship between the flow pattern of the pulp of the spiral concentrator and the roughness of the spiral groove surface and the viscosity of the pulp. Zhou Xiaohong [7] explored the effect of roughness on the slurry flow characteristics and particle separation behavior with the help of CFD spiral flow field model and particle phase calculation model. In this paper, with the help of CFD technology, three kinds of cross sections, namely "cubic parabolic", "elliptic" and "elliptic-cubic parabolic composite" (referred to as "composite"), are constructed respectively. Composite") three kinds of cross-section shape curve of the spiral concentrator CFD model, and with the help of the constructed model for the simulation of the flow state, to explore the different cross-section shape of the spiral concentrator sorting flow field of the influence of the flow state.

2 Modeling of Three Cross-sectional Spiral Groove Structures

2.1 Design of Cross-section Curves

In order to facilitate the experimental verification in the laboratory, this paper takes the spiral concentrator with outer edge diameter of spiral groove D=600mm, inner edge diameter d=110mm, pitch of h=270mm (pitch-to-diameter ratio h/D=0.45), and the number of laps as 5 as the object of study.

(1) Elliptical cross-section curve design

The equation of the curve is given in equation (1):

$$\frac{x^2}{a^2} + \frac{y^2}{b^2} = 1 \quad (1)$$

The shape is shown in Fig. 1.

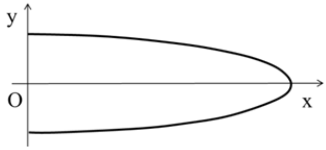

Fig. 1. Elliptic curve

(2) Cubic parabolic cross-section curve design

The equation of the curve is given in equation (2):

$$x = my^3 \quad (2)$$

The shape is shown in Fig. 2.

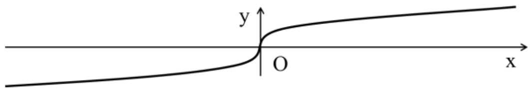

Fig. 2. Cubic parabolic curve

(3) "Elliptic-cubic parabolic" composite cross-section curve design

Generally speaking, elliptic is suitable for the recovery of coarse-grained minerals, while cubic parabolic is suitable for the recovery of fine-grained minerals, in order to improve the adaptability of the spiral concentrator, this paper proposes a spiral groove in the inner half (in the radial position of R = 122.5mm for the demarcation point) using elliptic curve, the outer half of the composite curve using cubic parabolic curve.

The equation of the curve is given in equation (3):

$$\mathrm{f(x)} = \begin{cases} \frac{x^2}{a^2} + \frac{y^2}{b^2} = 1, & x \in [0,122.5] \\ x = my^3, & x \in (122.5,245] \end{cases} \quad (3)$$

The shape and 3D model of the composite curve section is shown in Fig. 3. Points A and C in the figure correspond to the inner and outer boundary points of the spiral groove, and line AC is the main part of the cross-section of the spiral groove; point B is the demarcation point of the composite spiral groove, and line AB corresponds to the elliptic curve, while line BC corresponds to the cubic parabolic curve. The y-axis corresponds to the center axis of the spiral concentrator, and a corresponds to the groove width of the spiral groove, which can be expressed as the difference between the outer radius of the spiral groove(R) and the inner radius(r).

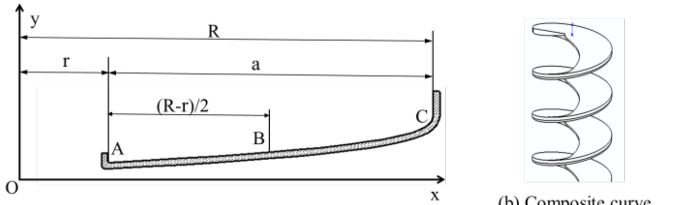

(a) Composite spiral groove cross section

(b) Composite curve section spiral concentrator

Fig. 3. Composite spiral groove cross section

3 Construction of CFD Model

(1) Mesh processing

Mesh quality and quantity directly affect the accuracy and speed of the control equation discretization in CFD numerical simulation, so appropriate high-quality mesh is the key to the numerical study of the flow field of the spiral concentrator. In this study, the ICEM module in ANSYS is used to perform hexahedral structured meshing of the computational domain. In order to accurately capture the flow field parameters near the boundary, five additional boundary layers are added in the region near the bottom of the trough and the side wall surface to improve the accuracy of the numerical simulation. The meshing of the cubic parabolic spiral concentrator is shown in Fig. 4, and the final number of meshes obtained is 1353100 with a minimum mesh quality of 0.6, which can meet the simulation requirements.

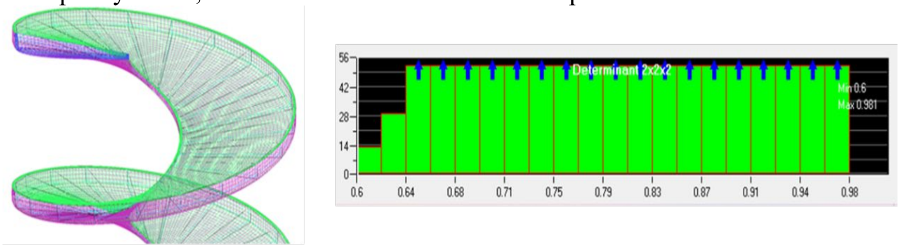

(a) Unstructured Mesh

(b)Mesh Quality

Fig. 4. Computational domain mesh processing

(2) Solver setting

In Fluent software, there are two numerical methods to choose from: the pressure-based solver (Pressure Based) and the density-based solver (Density Based). The Pressure Based solver is suitable for solving low velocity incompressible flows, while the Density Based solver is suitable for solving high velocity compressible flows. In the spiral concentrator, the fluid flow rate is generally in the range of 0-3m/s, which belongs to the low-speed incompressible flow, so the pressure-based solver is chosen for the solution calculation.

The pressure-based solver contains four separation and coupling algorithms, namely SIMPLE, SIMPLEC, PISO and Coupled, of which the first three are separation algorithms and the last one is coupling algorithm. Among them, SIMPLE algorithm is one of the most widely used algorithms, which predicts the new value of the velocity field by the given initial pressure and velocity, and then updates the pressure field according to the new value of the velocity, and then iterates so as to approach the real flow field situation continuously. After comprehensively considering the existing computational resources, accuracy and stability, SIMPLE algorithm is used for simulation in this paper.

(3) Multiphase flow model and turbulence model selection

When dealing with the spiral concentrator flow problem, since the flow presents an open liquid surface, unlike the pipeline flow, the fluid is in direct contact with the air, forming an obvious phase interface. This characteristic makes the use of the VOF model more appropriate than other models, which can better capture the dynamic features of the liquid surface morphology and interface changes.

For the spiral concentrator, the inner edge is dominated by laminar flow while the outer edge is dominated by turbulent flow, so the introduction of a suitable turbulence model can help to improve the reliability and accuracy of the simulation results.The RNGk-ε model in Fluent, which is used for the wall flow and in the case of a low mean pressure gradient, agrees well with the experimental results and is widely used in the study of the flow field with low to medium Reynolds number, so the RNGk-ε model is chosen in this study. RNGk-ε turbulence model is chosen for this study.

(4) Boundary conditions and computational domain initialization

In the numerical simulation of the fluid in the spiral concentrator, the boundary conditions are the physical quantities that need to be satisfied by the governing equations of the fluid dynamics at the boundary of the computational domain, and the reasonable setting of the boundary conditions is crucial to the accuracy of the simulation results.

In this simulation, the computational domain of the spiral concentrator is regarded as a mixture of water and gas phases, and there are four boundaries in the computational domain: the inlet, the outlet, the bottom of the tank, and the free-slip plane (which is in contact with the air throughout the whole process). The inlet adopts the velocity-inlet boundary condition, the velocity is obtained by the ratio of the inlet flow rate and the inlet area size, according to the existing research results of the team, the single-head fluid volume processing capacity of BL600 is $1m^3/h$; the outlet is set as the pressure-outlet, the pressure value is the standard atmospheric pressure, and the return volume of air is 1. The bottom of the computational domain and the outlet are set as the pressure outlet, the pressure value is the standard atmospheric pressure, and the return volume of air is 1. The bottom and side of the computational domain are set as no slipwall because of no energy exchange and impermeability; for the top of the computational domain, the top is set as free liquid surface in order to be closer to the actual spiral concentrator working without the upper wall. Before the numerical calculation, the flow field needs to be initialized, and reasonable initial conditions will accelerate the convergence speed. In the initial state, the computational domain is filled with air, the water flow enters the spiral chute from the inlet boundary, and the inlet is set as the water phase volume fraction of 1.

4 Analysis of Simulation Results

According to the existing experience, the mineral particles have basically completed 85% of the sorting when passing through the third circle of the spiral concentrator, so the flow field characteristic data at the end of the third circle is selected for comparative study and analysis.

4.1 Thickness of Flow Film

The thickness and unfolding width of the flow film of the spiral concentrator will directly affect the distribution of the ore particles, and the cloud diagrams of the distribution of the water phase as well as the thickness of the flow film under different cross-sectional shapes are shown in Fig. 5.

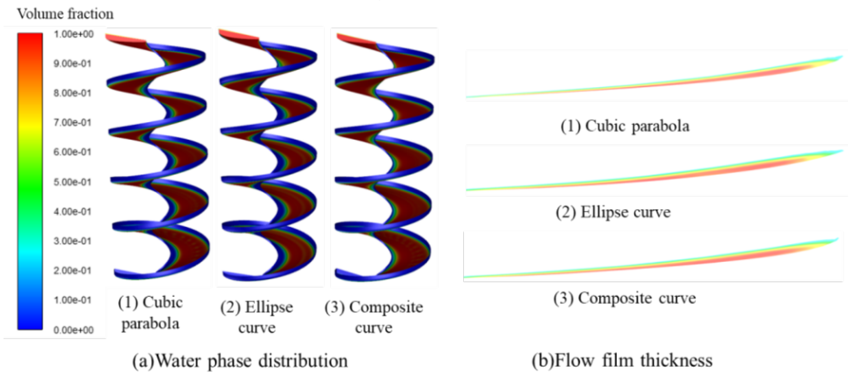

Fig. 5. Cloud diagram

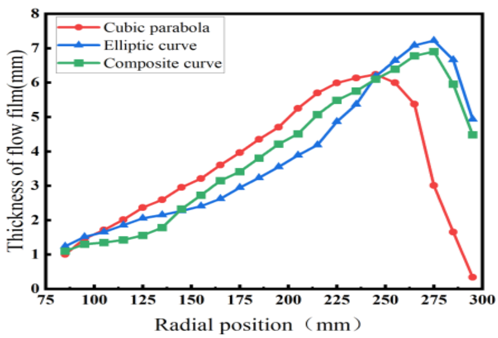

Fig. 6. Flow film thickness distribution

As can be seen from Fig. 5 and Fig. 6, the flow film thicknesses in all the three cross-sectional helical grooves show a regular spreading distribution state with thin inner edge and thick outer edge. Comprehensive Fig. 6 and Table 1 can be seen, the three flow film thickness in the radial position of 240mm to reach the same position, and this position to the inner edge, the elliptical cross-section of the flow film thickness is the largest, in the radial position of 140~240mm, the composite curved cross-section of the flow film thickness is greater than the cubic paraboloid, and the radial position of 140mm, the composite cross-section of the minimum thickness of the flow film. Generally speaking, a thicker flow film can provide a relatively stable sorting environment for coarse particles, so that they can be stratified and separated according to their own physical properties (such as particle size, density, etc.) in the flow film, however, it is not conducive to the settling and sorting of fine particles; on the contrary, in a thin flow film, the flow of the fluid is relatively smoother, and the fine particles are subjected to less interference, and it is easier for them to settle under the action of gravity, etc., but it also makes the coarse However, it also enhances the tendency of coarse minerals to move to the outer edge. From the simulation results, the overall film thickness of the composite curve cross-section is relatively moderate, which can not only ensure the effective settlement of fine particles, but also avoid the situation that coarse particles can not be deposited at the inner edge due to the thin film, which improves the recovery efficiency of coarse particles.

Table 1. Distribution of flow film thickness

Sectional curves	Radial position 125mm	Radial position 200mm	Radial position 275mm
Cubic parabola	2.06mm	3.89mm	7.22mm
Elliptic curve	2.37mm	5.25mm	3.01mm
Composite curve	1.55mm	4.51mm	6.91mm

4.2 Reynolds Number

Reynolds number is an important hydrodynamic parameter for judging the fluid flow pattern, and its variation has a significant effect on the sorting of minerals.

Similarly, we take the flow pattern at the end of the third circle as the object of study, and the comparison of the Reynolds number of the fluid at the end of the third circle of the spiral chute of three cross-sections is shown in Fig. 7, from which it can be seen that the Reynolds number of all cross-sectional shapes shows the tendency of increasing and then decreasing in the outward direction along the radial direction. The fluid flow in the spiral concentrator is similar to the open channel, according to the experience, the critical Reynolds number of laminar flow and turbulent flow is 500 and 1000 respectively, and the flow pattern between the two is defined as transitional flow. Comparing the distribution range of laminar flow region (Reynolds number <500) in the slot corresponding to the three different cross-section curves in the figure, the radial range corresponding to the elliptical cross-section is 85-155 mm, and the width of laminar flow region is 70 mm; the radial range corresponding to the cubic parabolic cross-section is 85-165 mm, and the width of laminar flow region is 80 mm; and the radial position corresponding to the composite curve cross-section is 85-175 mm. The width of laminar flow area is 90mm. It can be seen that the laminar flow area of the spiral groove with composite cross-section is the widest, and the fluid flow in the laminar flow area is relatively smooth, and the fine-grained minerals are less disturbed in such an environment, which is more favorable for their settling. Comparison of the range of transition flow area, the Reynolds number of elliptical cross-section spiral groove is obviously larger than the other two, and this area is the thickest mineral particle layer, the large enough Reynolds number of elliptical cross-section spiral groove is a guarantee of the loosening and separating of the coarse particle mineral layer. Comparing with the distribution of the film thickness, it can be found that the distribution of the corresponding Reynolds numbers in the three cross-sections is similar to the distribution of the film thickness. Therefore, from the analysis of the Reynolds number simulation results, it can be found that in the central part of the spiral chute where the mineral particles are dense, the elliptical cross-section spiral chute has a large enough Reynolds number and the thickness of the flow film, which is conducive to the sorting of coarse-grained minerals in the stratified layer, but is not conducive to the recovery of fine-grained minerals in the sedimentation. The composite curved cross-section spiral chute has the widest laminar flow area, which is more favorable to the separation and recovery of fine-grained minerals.

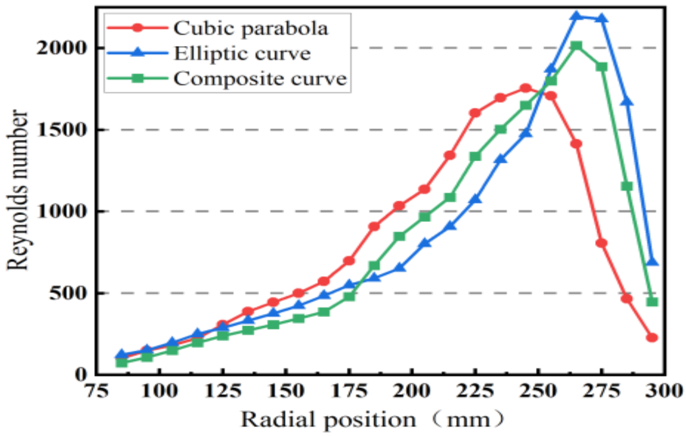

Fig. 7. Reynolds number distribution

4.3 Tangential Velocity

In the spiral chute, the main stream of the slurry is a downward rotary motion, and its tangential velocity determines the magnitude of the centrifugal force on the solid particles, and the kinetic energy of the fluid is transferred to the dispersed-phase solid particles, which affects the migration behavior of the particles. The distribution trend of tangential velocity along the radial direction for spiral concentrators with different cross-section curves is shown in Fig. 8.

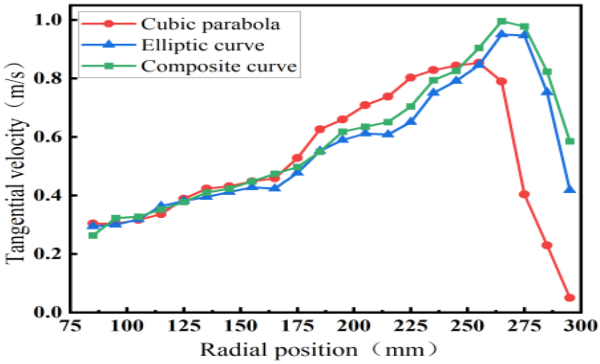

Fig. 8. Tangential velocity distribution

From the figure, it can be seen that the overall distribution of the tangential velocity of the three cross-sectional shapes of ellipse, cubic parabola and composite curve is similar to the distribution of the thickness of the flow film, and the thicker the film is, the weaker the viscous effect of the fluid on the groove surface is, and thus the larger the tangential velocity is. In the inner edge region, the distribution of the tangential velocities of each cross-section shape along the radial direction almost overlaps, indicating that the change of the cross-section shape does not have much effect on the radial velocity of the inner edge; with the increase of the radial distance, the ellipse's tangential velocity shows a rapid growth, and takes the lead to reach the peak value close to the outer side of the helical groove, while the composite cross-section and cubic-parabolic cross-section show a fluctuating growth in the central and outer edge region, and after the peak value, due to the effect of the sidewalls, the The tangential velocity of the fluid falls back near the outermost edge. At the same time, the tangential velocity is also the main reason for the secondary circulation phenomenon, in the case of the composite curve cross-section, the maximum tangential velocity value and the range, which becomes a necessary precondition for the subsequent enhancement of the intensity of the secondary circulation and the expansion of the circulation range.

4.4 Radial Velocity

Transverse secondary circulation is a phenomenon unique to the spiral concentrator, and is an important guarantee for the realization of mineral banding along the radial direction of the spiral groove according to the specific gravity. Its strength and scope directly affect the fluid's handling, stratification and banding of mineral particles along the radial direction. In order to facilitate the analysis, we use the measurement point from the bottom of the trough distance h and the ratio of the thickness of the flow film H defined as the relative depth of water and as the horizontal coordinate, assuming that the radial direction of the spiral groove from the inner edge to the outer edge of the movement is positive, from the outer edge of the movement to the inner edge of the direction of the movement is negative, then the different cross-sectional shapes of the spiral groove at the end of the third turn of the radial velocity of the fluid along the depth of the distribution as shown in Fig. 9.

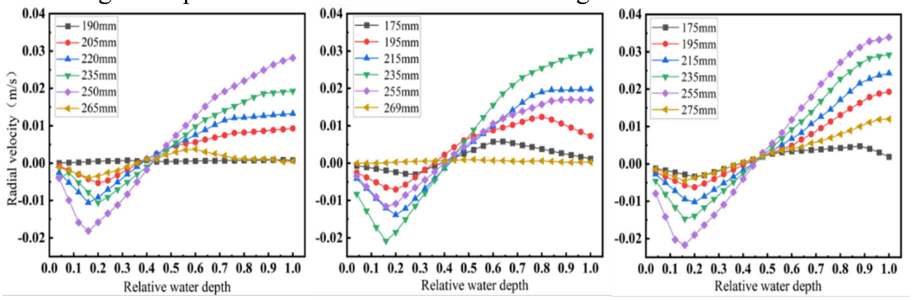

(1) Cubic parabola (2) Ellipse curve (3) Composite curve

Fig. 9. Radial velocity distribution of spiral concentrator with three cross-sectional shapes

As can be seen from the figure, above the relative water depth of 0.15, the fluid radial velocity increases with the increase of the relative water depth (i.e., the measurement point is gradually raised from the bottom of the tank to the liquid surface). In the relative water depth of 0.5 or less, the fluid flow rate is negative, that is, the fluid under the action of gravity from the outer edge to the inner edge of the movement; in the relative water depth of 0.5 or more, the fluid flow rate is positive, the fluid in the centrifugal inertia under the action of the inner edge of the movement to the outer edge of the formation of the secondary circulation phenomenon. At a relative water depth of 0.15, the lower fluid flow velocity reaches its maximum value, while the upper fluid reaches its maximum value at the liquid surface. There also exists a 0-velocity demarcation layer in the flow layer, in which the fluid moves neither outward nor inward. The secondary circulation is mainly concentrated in the region of the middle and outer edges, and its intensity increases and then decreases with the increase of the radial position. From Table 2, it can be seen that the range of secondary circulation is largest for the composite shaped cross section and smallest for the cubic parabolic. Relative to the cubic parabolic, elliptical cross-section, composite curve cross-section of the upper fluid maximum radial velocity value is the largest, to a certain extent, conducive to the lateral transport of mineral particles, but also reduces the chances of low-density particles into the inner edge of the spiral concentrator is conducive to improving the grade of the product of the inner edge of the spiral concentrator.

Table 2. Distribution of secondary circulation

Sectional curves	Radial position of secondary circulation		Range of secondary circulations
Cubic parabola	Initial	190mm	75mm
	Strongest	250mm	
	End	265mm	
Elliptic curve	Initial	175mm	94mm
	Strongest	235mm	

	End	269mm	
Composite curve	Initial	175mm	100mm
	Strongest	255mm	
	End	275mm	

5 Experimental Validation of CFD Model Simulation Results

In order to prove the reliability of the model and simulation results, this paper utilizes the laboratory experimental system of BL600 (spiral chute diameter φ600mm) spiral concentrator for experimental verification of the flow pattern. The thickness of the flow film at the end of the third lap was measured by an ultrasonic sensor, and these experimental data were compared with the simulation results. The measurement principle of the experimental system is shown in Fig.10(a). Before starting the experiment, a reference point P_1 at the bottom of the spiral chute was first determined, and the distance from this point to the sensor L_1 was recorded. When the fluid flow reached a steady state, the position P_2 of the free liquid surface and its corresponding distance L_2 were then marked. By calculating the difference between L_1 and L_2, the thickness of the flow film at the radial position was obtained, H. Based on the BL600 spiral concentrator's The distribution of the flow film thickness obtained from the actual test as well as the simulation is shown in Fig. 10(b).

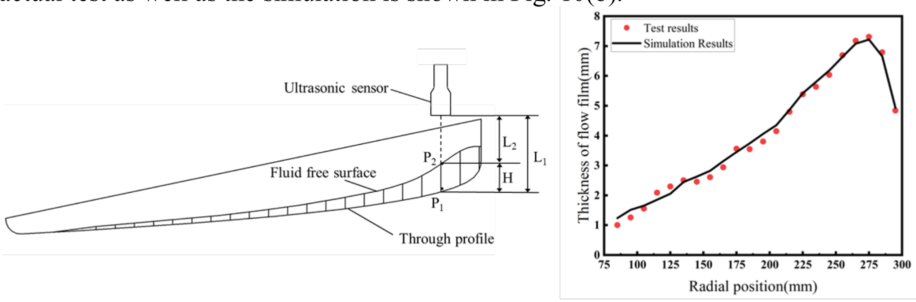

(a)Water phase distribution (b)Flow film thickness

Fig. 10. Measurement principle

From the comparison results in Fig.10(b), it can be seen that the laboratory measured results are more consistent with the simulation results of the CFD model, and the relative error rate MRE is 4.92%. The results indicate that the CFD model and simulation results established in this paper are reliable.

6 Conclusions

In order to explore the relationship between different cross-sectional shapes and the sorting fluid flow pattern of the spiral concentrator, this paper constructs three kinds of cross-sectional shapes of the spiral concentrator CFD model, and carries out the simulation simulation of the fluid flow pattern in the trough, and obtains the following conclusions:

(1) The overall flow film thickness of the composite curve cross-section is relatively moderate, which ensures the effective settling of fine-grained minerals and facilitates the deposition of coarse particles at the inner edge, thus enhancing the recovery of coarse-grained fine minerals.

(2) The simulation of Reynolds number found that in the middle of the spiral chute where the mineral particles are densely packed, the Reynolds number of the fluid in the elliptical cross-section spiral chute is larger, which is favorable to the sorting of coarse particles but unfavorable to the recovery of fine particles. This is also in line with our application experience. The spiral chute with composite curve cross-section has the widest laminar flow area, which is more favorable to the sorting and recovery of fine-grained minerals.

(3) Simulation of the radial velocity of the fluid in the spiral groove reveals that the composite shaped cross-section has the largest range of secondary circulation, which to some extent facilitates the lateral transport of mineral particles.

(4) In this paper, with the help of CFD technology on the influence of the shape of the cross-section of the spiral groove and the fluid flow in the groove, it is found that the shape of the cross-section of the spiral groove has a direct influence on the thickness of the film of the fluid flow in the groove, the tangential velocity, the Reynolds number, and the secondary circulation, and it will correspondingly affect the sorting behavior of the mineral particles and the sorting efficiency of the spiral concentrator.

Reference

1. Liu, H.Z. (2011) Progress and prospect of application of re-election equipment in metal ore dressing in China. Nonferrous Metals (Mineral Processing Section), 10: 18-22. 10.3969/j.issn.1671-9492.2011.z1.002.
2. Kapur, P., Meloy, T. (1999) Industrial modeling of spirals for optimal configuration and design: spiral geometry, fluid flow and forces on particles. Powder Technology, 102: 244-252. https://doi.org/10.1016/S0032-5910(98)00214-9.
3. Robben, C., Wotruba,H. (2019) Sensor-based ore sorting technology in mining—past, present and future. Minerals, 9: 523. 10.3390/MIN9090523.
4. Fan, X., Li, Z. (1974) Spiral chute—new equipment for separation of micro fine grade ores. Nonferrous Metals(Smelting), 6: 4-11+15. CNKI:SUN:METE.0.1974-06-001.
5. Sudikondala, P., Mangadoddy, N., Tripathy, S.K. (2023) CFD Modelling of the Spiral Concentrator at Moderate Feed Solids Content-Prediction of Particle Segregation. Transactions of the Indian Institute of Metals, 2023: 1-12. 10.1016/j.mineng.2022.107570.
6. Liu, H.Z., Zhu, H.J., Rui, B. (2024) Effect of flow resistance on the sorting flow field of spiral chute. Nonferrous Metals(Mineral Processing), 3:107-114. DOI:10.3969/j.issn.1671-9492.2024.03.013.
7. Zhou, X.H.,Gao, S.L.,Meng, L.G. (2023) Effects of wall roughness on slurry flow and particle separation behavior in spiral chute. Journal of Northeastern University (Natural Science Edition), 44(12):1769-1777. DOI:10.12068/j.issn.1005-3026.2023.12.013.